JMEPEG (2009) 18:1285–1293
DOI: 10.1007/s11665-008-9323-4

1059-9495/$19.00

Phase Transformations in Cast Superaustenitic Stainless Steels

Nathaniel S.L. Phillips, L. Scott Chumbley, and Brian Gleeson

(Submitted August 22, 2008)

The goal of this investigation was to study phase transformations in cast superaustenitic stainless steels. Experiments were performed to determine the phase transformation behavior for alloys CN3MN and CK3MCuN. Samples were taken from keel bars that were heat treated between 1160 and 1230 °C and then isothermally held for times ranging from 1 min to 2040 h at temperatures in the range of 700-900 °C. The resulting microstructures were characterized using scanning electron microscopy (SEM), transmission electron microscopy (TEM) and energy and wavelength dispersive spectroscopy. The microstructures, composed primarily of sigma- and Laves-phases within a purely austenitic matrix, showed relatively slow transformation kinetics, with transformation not completed even after the longest anneals. SEM and TEM analysis of superaustenitic samples reveal that precipitation takes place initially on grain boundaries and proceeds intragranularly. The results of these SEM and TEM investigations, along with volume fractions and number densities as a function of time and temperature, will be presented and discussed.

Keywords intermetallics, stainless steel, transformation kinetics

1. Introduction

Superaustenitic stainless steels are Fe-based systems highly alloyed with Cr, Ni, Mo, and N to produce excellent pitting and crevice corrosion-resistant properties at high temperatures and in seawater (Ref 1-5). When exposed to elevated temperatures for long periods of time, large amounts of precipitates, including carbides, nitrides, and intermetallic phases, can form in these steels (Ref 1-5). The most commonly observed secondary phases include $M_{23}C_6$ carbide, and intermetallic σ, χ, and Laves phases (Ref 1-5). Other less common secondary phases include M_6C, π, R, and Cr_2N (Ref 1-5). High amounts of these phases inhibit the corrosion resistance and mechanical properties of the stainless steels.

The type of precipitate strongly depends on the local composition and heating time and temperature. At temperatures ranging from 700 to 1100 °C, carbides are usually the first to form (Ref 1). At longer times, these carbides are usually replaced by intermetallic compounds, such as σ, χ, and Laves (Ref 1). Low carbon solubility has been found in σ, while a high solubility of interstitial elements in the austenite (γ) matrix tends to favor the formation of χ and Laves phases (Ref 1). Increased Mo percentages favor the precipitation of intermetallics at higher temperatures. High amounts of N (0.5 wt.%) have been found to prevent the χ phase from forming at all; rather, the formation of the Laves phase is reported (Ref 1, 3). However, the Laves-phase formation is delayed with additional N (Ref 1). Thus, the addition of N not only increases the mechanical properties of these materials, but also proves useful in delaying, or even preventing, harmful precipitates from ever forming.

There has been a large amount of research on the mechanical and corrosion-resistant properties of superaustenitic stainless steels (Ref 1, 2, 4, 5). However, little work has been done on determining the transformation kinetics of the matrix to form secondary phases at different temperatures, and what has been done relates predominantly to wrought alloys (Ref 3). Differences in the phase transformation kinetics between cast and wrought alloys, which are presumably due to discrepancies in the nominal composition, have been documented (Ref 6). It is the focus of this paper to examine the transformation behavior in cast superaustenitic steels, particularly in regards to the formation of the σ and Laves phases, since they appear to be the most abundant. This paper contains phase characterization and transformation behavior results for the cast superaustenitic alloys CN3MN and CK3MCuN. Following quenching and isothermal holds, quantitative analyses using standard metallurgical techniques were performed to identify phases and their volumes percentages.

2. Experimental Procedure

Two heats each of CN3MN and CK3MCuN in the form of $3 \times 4 \times 35$ cm keel bars were received for examination in the solution heat-treated condition, with the heat treatment being between 1160 and 1230 °C (2125 and 2250 °F) for at least 2 h. Measured nominal compositions of the alloys studied are given in Table 1.

Samples were heat treated between 600 and 900 °C from 1 min to 2040 h. Short-term heat treatments (up to 500 h) were performed by transferring the sample directly from the vertical tube furnace to a salt bath. Longer heat treatments were performed in box furnaces.

Nathaniel S.L. Phillips, L. Scott Chumbley, and **Brian Gleeson**, Iowa State University, 214 Wilhelm, Ames, IA 50011. Contact e-mails: phillips_nate@cat.com, chris.c.muller@gmail.com.

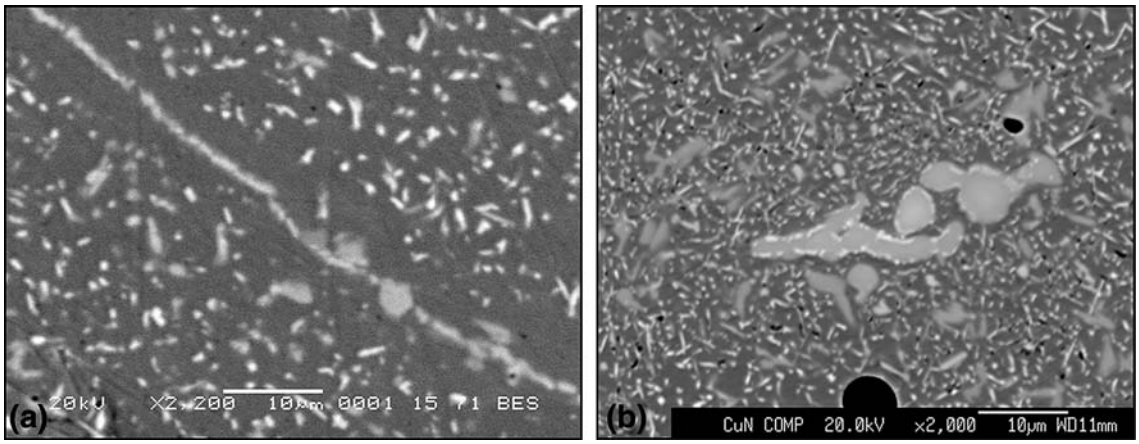

Fig. 1 Backscattered images of CK3MCuN after 850 °C for 500 h (left) and 800 °C for 500 h (right)

Table 1 As-received compositions for CN3MN and CK3MCuN keel bars

	CN3MN	CK3MCuN
C	0.023	0.025
Si	0.74	0.90
Mn	0.59	0.73
P	0.013	0.015
S	0.004	0.007
Cr	20.9	20.2
Mo	6.5	6.6
Ni	24.6	17.7
Cu	0.12	0.53
N	0.22	0.20

Samples for characterization were prepared using standard metallographic techniques. The transformation kinetics and resulting phases were analyzed with optical microscopy, scanning electron microscopy (SEM), energy-dispersive spectroscopy (EDS), and wavelength-dispersive spectroscopy (WDS). The center region of the samples was examined to avoid any surface effects, and numerous images of each heat treatment were taken from randomly selected areas for determining volume fraction and number densities. More definitive characterization was carried out with transmission electron microscopy (TEM), with diffraction patterns obtained from the various phases being analyzed and compared to literature data. TEM samples were prepared using a jet polisher. The solution used was 5% perchloric acid in 25% glycerol and 70% ethanol at −20 °C and a potential of 50 V. An EDS system attached to the TEM was used as an initial screening of possible phases.

3. Experimental Results

3.1 CK3MCuN

Contrast variations in backscattered electron (BSE) images made it possible to differentiate between phases due to atomic number differences. Precipitation of intermetallic phases was found after heat treatments at low temperatures (700 °C) and short soak times (1 min) in CK3MCuN. Figure 1 shows examples of typical microstructures observed after long aging times. While precipitation starts along the interdendritic boundaries, growth continued both at the boundaries and homogeneously within the dendrites as heat treatment times and temperatures increased. A coarsened gray phase is first seen along the interdendritic boundaries; shortly thereafter a needle-like white phase precipitates.

Table 2 Microprobe WDS results for CK3MCuN after 500 h at 900 °C

Composition, wt.%						
Si	**Fe**	**Mo**	**Cr**	**Ni**	**Mn**	**Phase**
2.6	40.7	28.0	17.2	10.5	0.5	White
1.4	42.6	12.8	31.9	9.7	0.6	Gray
0.9	57.0	2.2	22.2	16.9	0.8	Matrix

Results obtained from WDS scans of several white and gray precipitates seen in the 900 °C, 500-h heat-treatment sample are presented in Table 2. (These quantitative compositions were used in comparison to the qualitative EDS compositions obtained during initial screening of phases to be identified with TEM.) TEM analysis of a CK3MCuN sample heat treated at 800 °C for 500 h confirmed that the high-Cr gray phase was σ and the high-Mo white phase was Laves. The diffraction results were compared to crystallographic information found in Table 3.

Metallographic examination of CK3MCuN samples showed a small amount of σ phase was present in the solution heat-treated samples before the isothermal hold. Nucleation of the σ phase was low until approximately 100 h at all temperatures, after which an increase in the number of precipitates was seen. Subsequent growth occurred very slowly, such that equilibrium was not reached at 700 and 800 °C even after the maximum heat-treatment time of 2040 h. Volume percents seen after this time are above 20%. The amount of σ at 900 °C leveled off at ~12%. Measured σ volume percentage data with error bars of one standard deviation are presented with a best-fit curve in Fig. 2.

Metallographic examination did not reveal any Laves present in the solution heat-treated structure. However, Laves was present after about 30 min at 900 °C and 500 h at 700 and 800 °C. The Laves phase reached a maximum of 4.6, 6.8, and

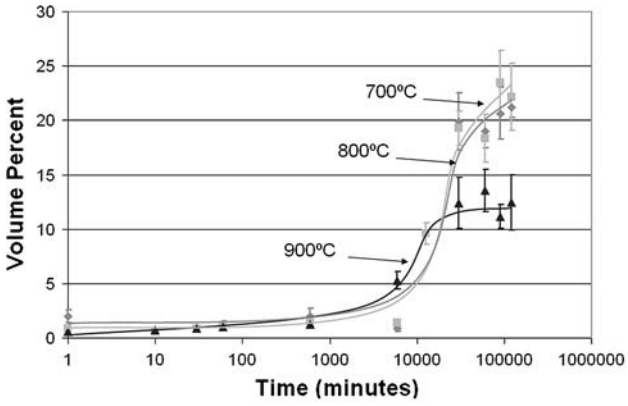

Fig. 2 Experimental σ volume percents and best-fit curve for CK3MCuN

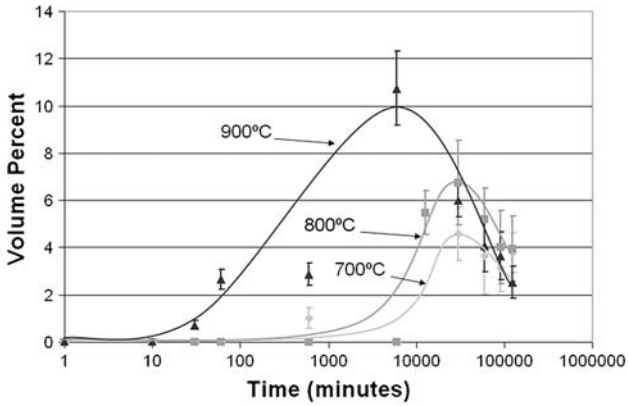

Fig. 3 Experimental Laves volume percents in CK3MCuN and best-fit curve

Table 3 Experimental and literature lattice parameters for σ and Laves in CK3MCuN

Phases	Lattice type	Experimental lattice parameter, Å	Literature lattice parameter[2], Å	EDS composition, wt.%
σ	BCT	a = 8.76, c = 4.57	a = 8.80, c = 4.54	23.6Fe-45Cr-16.3Ni-12.6Mo
Laves	HCP	a = 4.74, c = 7.70	a = 4.744, c = 7.725	25.4Fe-11.5Cr-7.4Ni-52.6Mo

10.0% at 700, 800, and 900 °C, respectively, at 500 h. The dissolution of Laves phase was apparent after 100, 250, and 500 h at 900, 800, and 700 °C, respectively. Measured Laves volume percentage data with error bars of one standard deviation are presented with best-fit curves in Fig. 3.

The contrast of phases in the BSE images also made it possible to calculate the number densities of σ and Laves for all heat treatments. The volume percentages are compared to the number densities for σ and Laves at 700, 800, and 900 °C in Fig. 4, which are shown plotted with one standard deviation error bars. Microstructures that correspond to these graphs can be found in Fig. 5.

3.2 CN3MN

Intermetallic phases similar to what were seen in CK3MCuN were observed at similar temperatures in CN3MN. Precipitation again was observed to first form along the interdendritic boundaries, although the scale of the precipitates was much finer than that of CK3MCuN for aging times up to 500 h. Phase characterization proved to be extremely difficult in this alloy due to the fine scale of the precipitates, which was below the spatial resolution of EDS and WDS using SEM techniques for accurate chemical analysis. TEM was used again to positively identify the phases in CN3MN. Both σ and Laves were found in a sample heat treated at 800 °C for 2040 h. The lattice parameters and EDS compositions of both phases were very similar to those found for σ and Laves in CK3MCuN (Table 3).

Unlike CK3MCuN, a significant amount of macrosegregation corresponding to the original cast dendritic structure was observed at all temperatures for all times (Fig. 6). At the longest times studied it was evident that growth of σ was favored in the former intradendritic regions while Laves was favored in the interdendritic regions. Compositional map scans using WDS revealed the macrosegregation of Mo in the solution heat-treated samples.

Metallographic examination of CN3MN showed that σ and Laves nucleated at longer times than for CK3MCuN. The interdendritic region (high Mo concentration) was observed to be favorable for Laves nucleation, while the intradendritic region (low Mo concentration) favored σ nucleation. At 900 °C, the microstructure seems to be completely σ for all times greater than 1000 h. Experimental volume percentage data for σ and Laves with error bars of one standard deviation are presented with best-fit curves in Fig. 7 and 8, respectively. It is apparent that the σ volume percent will continue to increase after 2040 h at all temperatures. The Laves phase dissolved at 800 and 900 °C after 1000 and 10 h with maximum volume percents of 5.3 and 6.6, respectively. The high amount of error associated with the volume percent measurements was a direct result of the observed macrosegregation.

The volume percentages and number densities for σ and Laves at 700, 800, and 900 °C are presented in Fig. 9. Error bars are once again high due to macrosegregation and the finer size-scale of the precipitates. Microstructures that correspond to these graphs are presented in Fig. 10.

4. Discussion

4.1 Microstructure Evolution

The microstructures for both alloys showed similar behavior at short heat-treatment times at all temperatures. However, due to segregation of Mo in CN3MN, the microstructures were very different for longer heat-treatment times. The σ phase initially formed along interdendritic boundaries and near voids for both alloys. There was a small amount ($<0.5\%$) of σ precipitation in the as-solution heat-treated structure for CK3MCuN, whereas it took between 30 and 60 min for σ to nucleate in CN3MN.

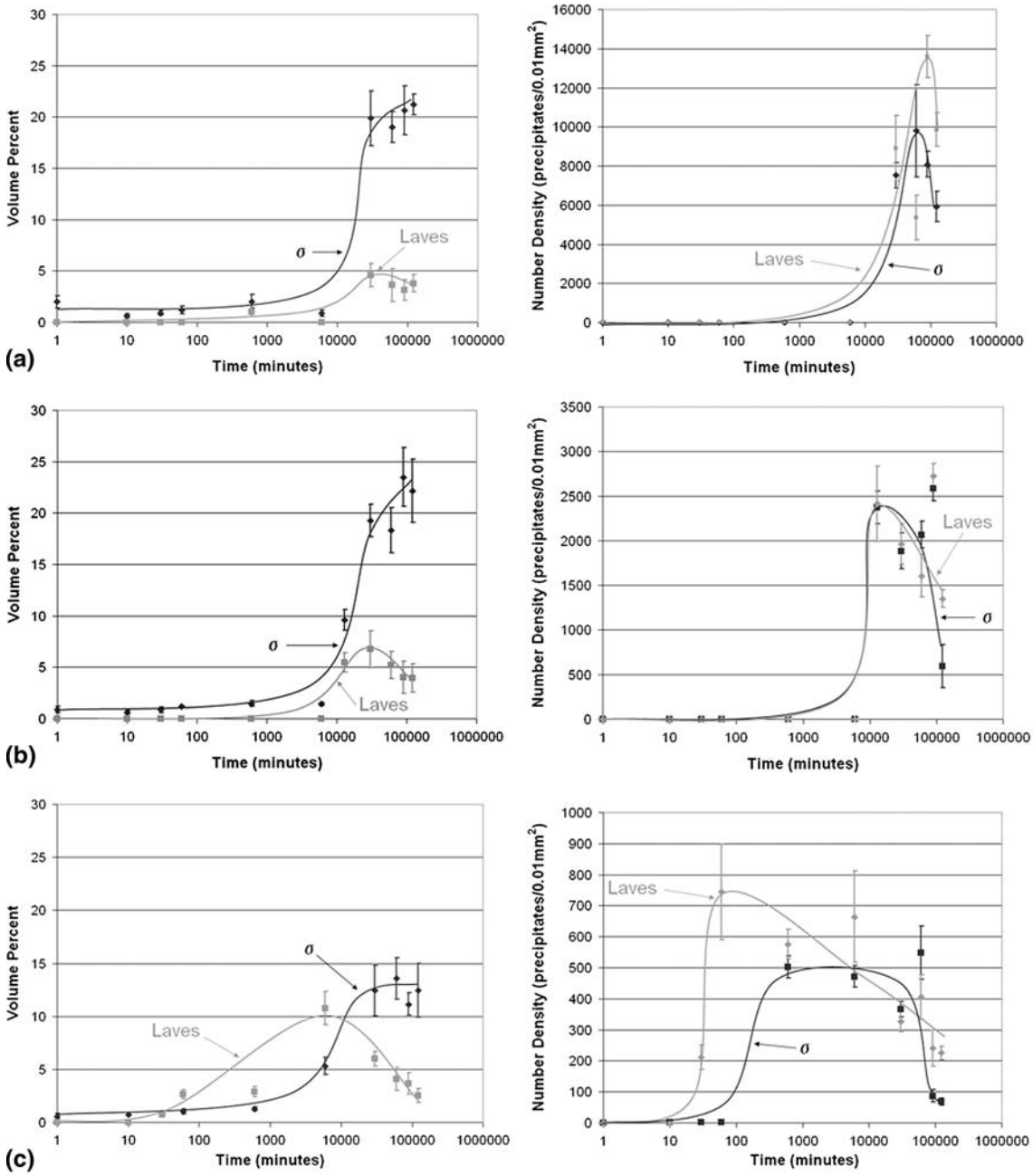

Fig. 4 Volume percents (left) and number densities (right) of σ and Laves at (a) 700 °C, (b) 800 °C, and (c) 900 °C in CK3MCuN

Laves formation followed that of σ formation. Initial precipitation occurred along the interdendritic boundaries and near voids, followed by intradendritic precipitation of very fine needle-like Laves. Laves particles on the interdendritic boundaries were always larger than the Laves particles that nucleated within the dendrites. Fine intradendritic σ precipitation usually followed the intradendritic precipitation of Laves. Similar to Laves, the intradendritic σ precipitates were much smaller in size compared to the σ found along the interdendritic boundaries and near voids. This explains the somewhat unusual observation that the average size of the particles was very high for short times but decreased as finer-scale σ and Laves started to nucleate within the grains. Once growth and coarsening of both phases commenced, the average size started to increase. In CN3MN, Laves was only seen in the interdendritic regions, where the high amounts of Mo segregation occurred. The intradendritic σ that nucleated in this alloy was in greater amount than in the interdendritic regions. At longer times (≥500 h), Laves was seen to nucleate on the σ throughout both alloys.

The maximum size of Laves particles was much larger in CK3MCuN than in CN3MN at all temperatures. The Laves precipitates in CK3MCuN became more spherical as time progressed, while they remained needle-like at all times in CN3MN. After the Laves reached a certain maximum amount, it started to dissolve back into solution. This was evident at all temperatures for CK3MCuN and at 800 and 900 °C in CN3MN. Laves dissolved completely at 900 °C for CN3MN. The maximum size of a Laves precipitate before it dissolved

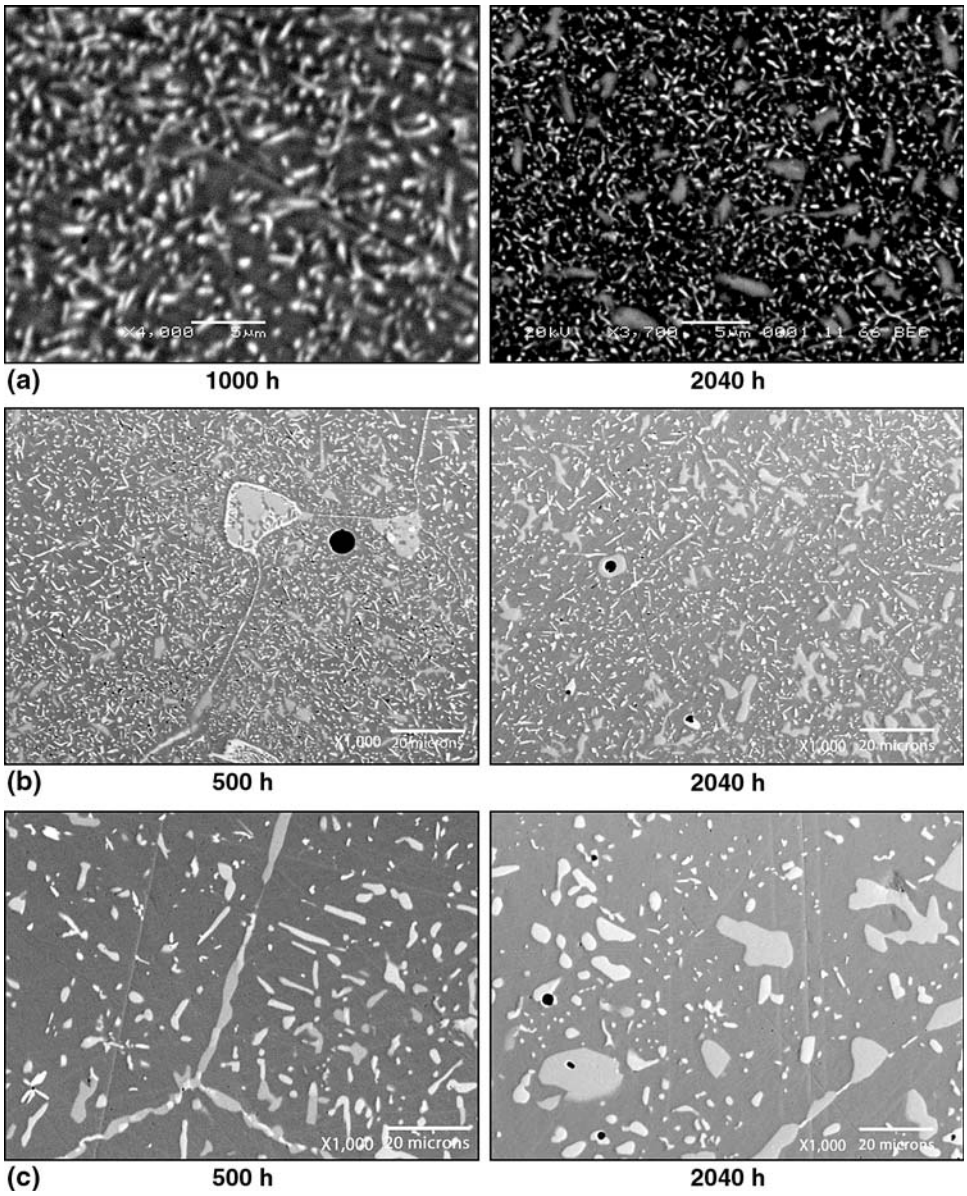

Fig. 5 BSE images of CK3MCuN at (a) 700 °C, (b) 800 °C, and (c) 900 °C

was never as large as the σ precipitation for the same time and temperature.

4.2 Volume Percents and Number Densities

The volume percent determinations, as presented in Fig. 2 and 7, reveal that the time needed to start nucleating σ along the interdendritic boundaries is much shorter in CK3MCuN than in CN3MN. However, the overall time required to nucleate σ intragranularly before it started to grow was shorter in CN3MN than CK3MCuN. Growth started after 10 h at all temperatures in CN3MN. Similarly, growth started after 10 h at 900 °C in CK3MCuN, but did not start until after 100 h at 700 and 800 °C. The rates at which σ grew in the two alloys were vastly different. In CK3MCuN, the σ volume percents apparently started to reach equilibrium at 900 °C after about 500 h. In contrast, the volume percents are still increasing at 700 and 800 °C up to the maximum heat-treatment time of 2040 h. The σ volume percents in CN3MN were still increasing at a steady rate up to 2040 h at all temperatures.

The time needed to nucleate Laves was similar at 700 and 900 °C in both alloys, as seen in Fig. 3 and 8. However, at 800 °C, the time needed to nucleate Laves was much longer in CK3MCuN. The time required to reach maximum growth at 900 °C in CK3MCuN is much longer than in CN3MN, while the times were quite similar for both alloys at 800 °C. However, Laves was still growing at 2040 h at 700 °C in CN3MN. An obvious dissolution of Laves occurred at all temperatures in CK3MCuN, while dissolution was only seen at 800 and 900 °C in CN3MN.

The number densities of both σ and Laves as a function of time for CK3MCuN reached a maximum, which would indicate the end of nucleation and the beginning of growth. For 700 and 800 °C, the number densities reached a maximum and then decreased due, in part, to the start of coarsening of both phases.

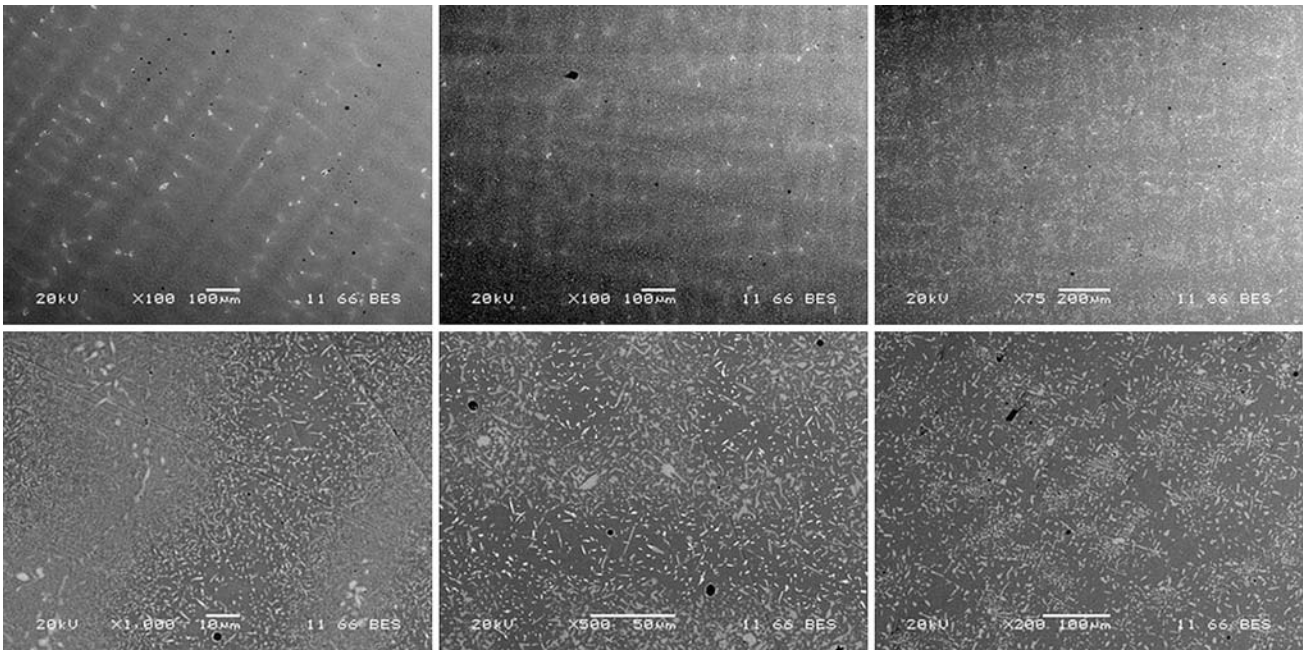

Fig. 6 Backscattered SEM images taken at low magnification (top) and high magnification (bottom) after 2040 h at 700 °C (left), 800 °C (middle), and 900 °C (right)

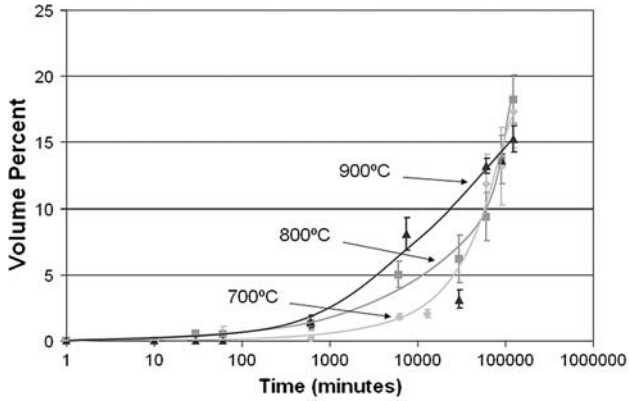

Fig. 7 Experimental σ volume percents and best-fit curve for CN3MN

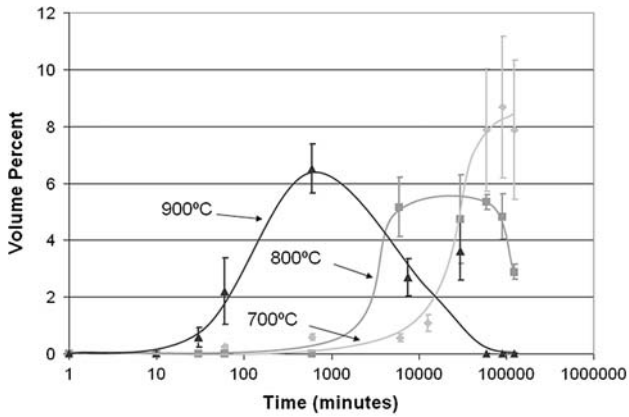

Fig. 8 Experimental Laves volume percents and best-fit curve for CN3MN

The number of Laves precipitates would also decrease as dissolution occurred. At 900 °C, a similar maximum was seen for Laves; however, the growth of σ occurred over a range of times before starting to coarsen. The number densities for CN3MN reveal that the number of Laves precipitates decreased at all temperatures, including 700 °C, as time increased. The overall number of σ precipitates was much lower than the number of Laves precipitates at 800 and 900 °C before dissolution occurs, even though the volume percents of σ were higher for the same times. Thus, the average size of a Laves particle was much smaller than the average size of a σ particle at all times. The number density of σ also appeared to increase at the same time the number density of Laves decreased at 800 and 900 °C. This would suggest that σ nucleation was a direct result of the Laves dissolution.

Based on the results from the volume percents and number densities of σ and Laves, several conclusions can be made. First, the system preferentially forms σ at longer times and therefore σ is considered to be the stable phase. Laves is considered to be a metastable phase in these systems since it dissolved into solution partially at most temperatures and completely at 900 °C in CN3MN. Metastability in this case assumes that a driving force for formation exists at the temperatures of interest, but the magnitude of that driving force is lower than what exists for the stable phase (i.e., σ). This is believed to be a result of the interfacial energy between the matrix and precipitate nuclei being less for the γ/Laves interface than the γ/σ interface. The interfacial energy between FCC-γ and HCP-Laves is assumed to be much lower than between FCC-γ and BCT-σ, since FCC and HCP are both closed-packed crystallographic structures. This has been suggested by Svoboda et al. (Ref 3), and is supported by the observations of this study where Laves was seen to dissolve into solution at all temperatures. It is also possible that Laves may come to an equilibrium state at temperatures where complete dissolution was not observed.

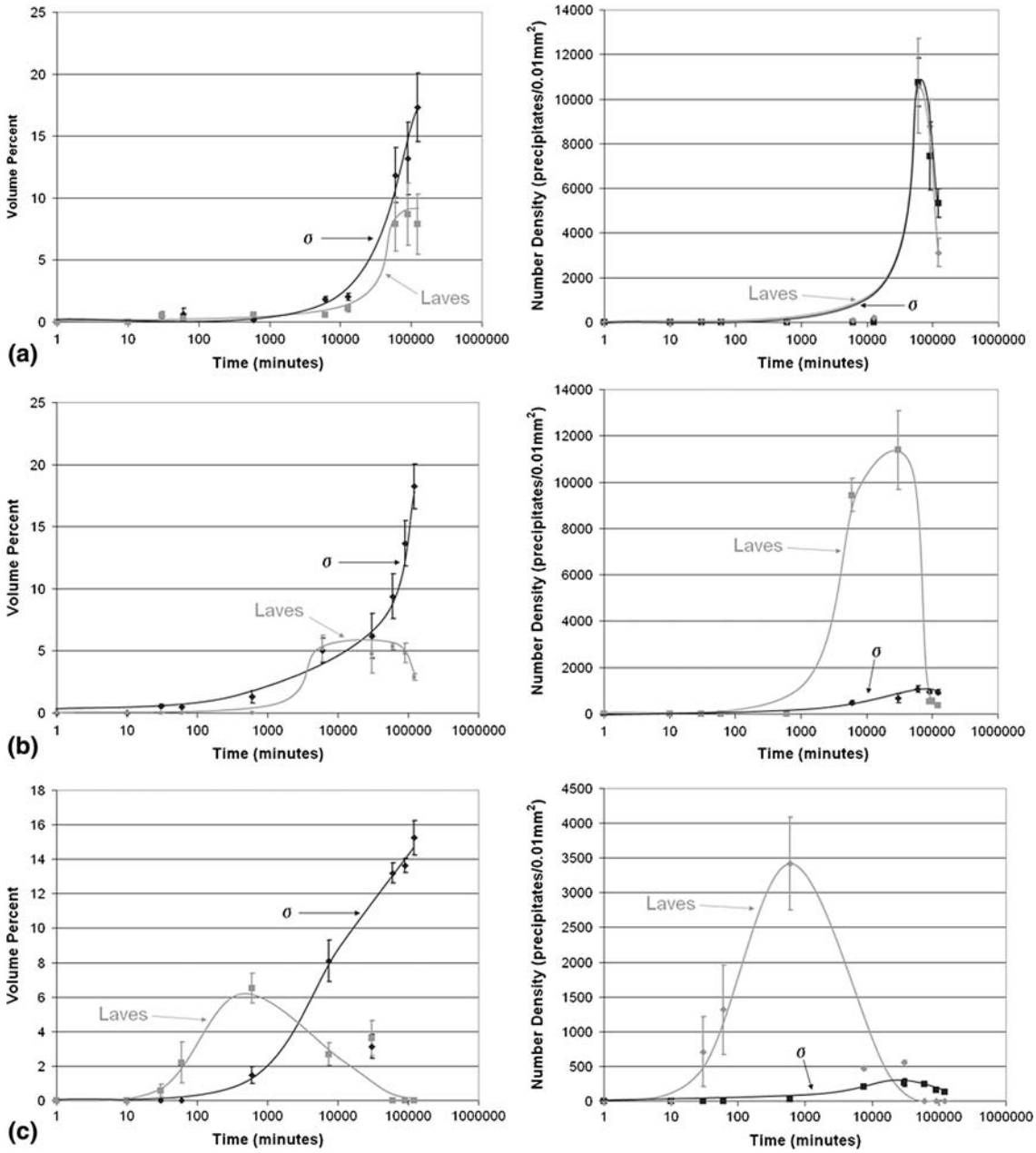

Fig. 9 Volume percents (left) and number densities (right) of σ and Laves at (a) 700 °C, (b) 800 °C, and (c) 900 °C in CN3MN

The fact that the number density of σ reached a maximum would lead to the conclusion that the system was at equilibrium. However, the volume percents were increasing at all temperatures and times at which the number density suggests equilibrium had been reached. Therefore, it appears that growth and coarsening of σ were occurring concurrently due to local composition differences. This is especially true in the case of CN3MN where σ was at a lower amount in the interdendritic regions due to macrosegregation of Mo. The favored formation of σ eventually causes the Laves to dissolve. The Cr and Mo provided by the Laves dissolution would diffuse toward the σ in the interdendritic regions and cause further growth of this phase. However, the dendritic regions may have reached uniform compositions locally, thus mitigating further growth and signaling the start of coarsening. This may be the reason why the growth of σ in CN3MN took much longer than in CK3MCuN. Also, the number densities were much larger and average particle sizes much smaller for Laves in CN3MN than in CK3MCuN. This suggests that Laves did not coarsen as much in CN3MN as in CK3MCuN.

5. Conclusions

Backscattered electron SEM images revealed an obvious contrast between two intermetallics and the austenitic matrix. Phase identification using TEM coupled with WDS measurements revealed BCT-σ and HCP-Laves phases, which formed at all temperatures studied in both alloys.

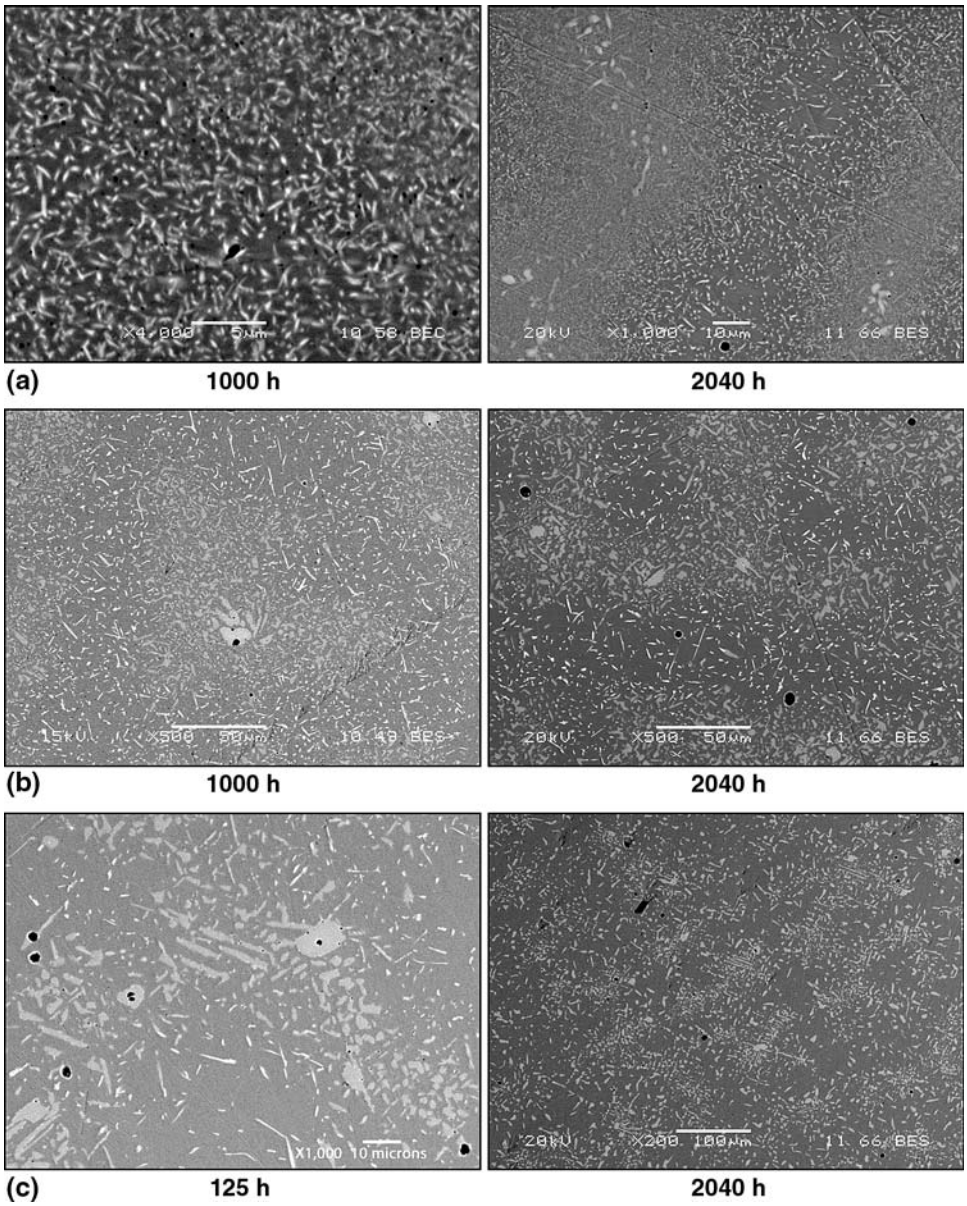

Fig. 10 BSE images of CN3MN at (a) 700 °C, (b) 800 °C, and (c) 900 °C

The transformation kinetics of both CN3MN and CK3MCuN were extremely sluggish. Equilibrium conditions were not reached in either alloy after 2040 h at 700-900 °C. The transformations occurred fastest at 900 °C, indicating the maximum transformation rate could be at temperatures higher than 900 °C.

Precipitation in CK3MCuN begins with the formation of high-Cr plate-like σ along the interdendritic boundaries and near voids. Shortly thereafter, the needle-like Laves formed intradendritically around the σ. Laves continued to nucleate within the dendrites and σ shortly followed.

Macrosegregation of Mo was seen in the cast and solution-treated samples of CN3MN. Laves formed only in high-Mo interdendritic regions, while higher σ amounts were found in the intradendritic regions than in interdendritic regions. Laves phase subsequently dissolved, indicating metastability. The stable σ phase continued to grow at the maximum heat-treatment time of 2040 h at all temperatures in CN3MN and at 700 and 800 °C in CK3MCuN. The σ at 900 °C in CK3MCuN stabilized at approximately 12 vol.%.

Intradendritic nucleation and growth of σ was much slower than the Laves, possibly due to a crystallographic orientation relationship between the HCP-Laves and FCC-γ. The nucleation and growth rate of Laves in CN3MN was much faster at 800 and 900 °C than in CK3MCuN. The nucleation rate of σ was also much faster in CN3MN; however, the growth rate was slower. The slow growth rate can be attributed to the segregation of Mo in the interdendritic regions, which made the formation of Laves preferential. The macrosegregation of Mo seen in CN3MN could have been avoided if the as-cast bars were solution heat treated at temperatures and times that allowed for complete dissolution of Mo.

Number density and volume percent studies indicated that growth and coarsening of σ occur simultaneously in both alloys. This phenomenon is assumed to be a result of local compositional differences.

Acknowledgments

The authors thank Malcolm Blair and Ray Monroe of the Steel Founders Society (SFSA) of America for their assistance and guidance in this study. We are also grateful to the various industry members of SFSA for providing samples, helpful discussions, and technical advice in conducting this research, especially Mr. Ron Bird. The assistance of Dr. Y.-J. Kim and C. Muller is also acknowledged. This research was supported by the US Department of Energy through a contract managed by Advanced Technology Inc.

References

1. S. Heino, Role of Mo and W During Sensitization of Superaustenitic Stainless Steel—Crystallography and Composition of Precipitates, *Metall. Mater. Trans.*, 2000, **31A**, p 1893–2904
2. S. Heino, M. Knutson-Wedel, and B. Karlsson, Precipitation in High Nitrogen Superaustenitic Stainless Steel, *Trans Tech Publications Ltd.*, 2005
3. M. Svoboda, A. Kroupa, J. Soousek, J. Vrest'al, and P. Miodownik, Phase Changes in Superaustenitic Steels After Long-Term Annealing, *Z. Metallkd.*, 2004, **95**, p 1025–1030
4. T.-H. Lee, S.-J. Kim, and Y.-C. Jung, Crystallographic Details of Precipitates in Fe-22Cr-21Ni-6Mo-(N) Superaustenitic Stainless Steels Aged at 900°C, *Metall. Met. Trans.*, 2000, **31A**, p 1713–1723
5. S. Heino, M. Knutson-Wedel, and B. Karlsson, Precipitation in a High Nitrogen Superaustenitic Stainless Steel, *Mater. Sci. Forum*, 1999, **318–320**, p 143–148
6. Y.-J. Kim, L.S. Chumbley, and B. Gleeson, Development of Isothermal Transformation Diagrams for Sigma-Phase Formation in Cast Duplex Stainless Steels, 2003 (Chicago), Steel Founders' Society, *Steel Founders' Society of America 2003 T&O Conference*, 2003